Deep Learning-based Stress Determinator for Mouse Psychiatric Analysis using Hippocampus Activity

DONGHAN LIU[1], **BENJAMIN C. M. FUNG**[2], **AND TAK PAN WONG**[3]

[1] *School of Information Studies, McGill University, Montreal, Canada, Email: donghan.liu@mail.mcgill.ca*
[2] *School of Information Studies, McGill University, Montreal, Canada, Email: ben.fung@mcgill.ca*
[3] *Douglas Research Centre, Montreal, Canada, Email: takpan.wong@mcgill.ca*

Decoding neurons to extract information from transmission and employ them into other use is the goal of neuroscientists' study. Due to that the field of neuroscience is utilizing the traditional methods presently, we hence combine the state-of-the-art deep learning techniques with the theory of neuron decoding to discuss its potential of accomplishment. Besides, the stress level that is related to neuron activity in hippocampus is statistically examined as well. The experiments suggest that our state-of-the-art deep learning-based stress determinator provides good performance with respect to its model prediction accuracy and additionally, there is strong evidence against equivalence of mouse stress level under diverse environments.

1. INTRODUCTION

Neural decoding is a discipline of studying the neural activity and transforming these potential recognized patterns to link with animal's motor activity. It is widely applied in various circumstances, such as mimic neuron activity to control the body movement or understand the signal or information that the neuron activity is transmitting. Stephen Hawking, for example, is unable to move his body or even speaking, nonetheless, it becomes possible if the neural decoding technique is well-developed so that his neuron activity can be used to control his wheelchair and speaker.

Having said that, the traditional method is still the main trend in the neural decoding field. With the rapid development of machine learning (ML), especially deep learning, we can treat neural decoding as an ML problem and use deep learning techniques to address it. On the other hand, the application of deep learning approaches varies by different types of purposes of studying neurons, such as predict motor activity, physical location, etc.. ML may be beneficial for advancing the potential to have better performance and deeper insight on neural function.

In addition to employ ML in neural decoding, we study the relationship between animals' stress level and its neuron activity. We aim to determine the significant difference in neuron activity in various environments. By studying it, we can observe whether the stress has an impact on the neuron activities, either enhance or weaken. It also tells us if the stressful or not neuron activity is the determining factor in the animal's motor activity. In this paper, we summarize the contributions as follows:

- We propose an idea of predicting animals' stress level by applying the state-of-the-art deep learning model
- We statistically prove that the stress level is significantly different under the various environments

2. RELATED WORK

Long-Short-Term-Memory (LSTM) [1], [2] have accomplished influential results in time-series forecasting [3], [4], [5]. Among the variants of LSTM, bi-directional LSTM [6] perform significantly impressive than the vanilla LSTM[7]. In the rest of the paper, we refer to the "bi-directional LSTM" as "BiLSTM" for simplicity. *BiLSTM* applied additional training to traverse the input data twice, from left to right (forward) and from right to left (backward), so in short, *BiLSTM* has more training power than the original un-bidirectional LSTM. In other words, it allows itself to preserve information from the future and combines two hidden states so that we are able in any point in time to preserve information from both past and future [6].

According to the visualization of LSTM cell [8], each of them consist of forget gate, input gate, cell gate, output gate, and activation functions of users' choice. We refer readers to original LSTM paper for more details [1].

Gated Recurrent Unit (GRU) [10] has similar theory with LSTM but slightly different architecture inside the GRU cell. It outperforms LSTM while the training dataset is small [10]. That being said, GRU is a better fit for our dataset size. However, without taking experiments into account, it is inappropriate to speak that LSTM is not as good as GRU in our case. The model's performance comparison in terms of our dataset is offered in the following paper. For the purpose of simplicity, we use LSTM to represent both LSTM and GRU in the network cell and model architecture because they share the same overall structure.

Support Vector Machine (SVM) [11] aims to find a hyperplane in an N-dimensional space that distinctly classifies the data

Fig. 1. LSTM cell [9]

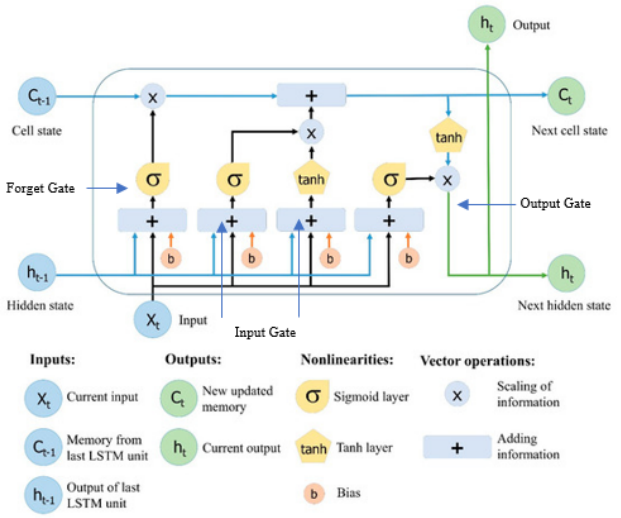

points, in other words, the objective of SVM is to find the decision boundary with maximum margin, from a mathematical perspective:

$$min_(w,w_0)||w||_2^2$$

$$y^n(wx^n + w_0) \geqslant 1 \forall n$$

where weights for the input features denote by w, and intercept denotes by w_0.

Random Forest [12] is a tree-based [13] algorithm, in which train numbers of decision trees and use *voting* technique of bootstrap aggregating (bagging) [14] to make the final classification. The method of features sub-sampling that embedded in Random Forest algorithm can reduce the variance of unstable models and further help the performance of models.

Naive Bayes [15] consist of three scenarios of input feature types: Bernoulli Naive Bayes, Multinomial Naive Bayes , Gaussian Naive Bayes. Among them, Gaussian Naive Bayes will be discussed as our input dateset follows continuous distribution. We assume the data in a normal distribution, which is formulated in:

$$p(x_d|y) = N(x_d; \mu_{d,y}, \sigma_{d,y}^2) = \frac{1}{\sqrt{2\pi\sigma_{d,y}}} e^{-\frac{(x_d-\mu_{d,y})^2}{2\sigma_{d,y}^2}}$$

where

$$\mu_{d,y} = \frac{1}{N_c} \sum_{n=1}^{N} x_d^n y_c^n$$

$$\sigma_{d,y}^2 = \frac{1}{N_c} \sum_{n=1}^{N} y_c^n (x_d^n - \mu_{d,y})^2$$

Student's t-test [16] is a statistical hypothesis test, where its test statistics follow the Student's t-distribution based upon the null hypothesis. The general use of Student's t-test is to determine if the means of two sets of data are significantly different from each other. There are several different cases for diverse data: equal sample sizes and equal variance; equal or unequal sample sizes and equal variance; equal or unequal sample sizes and unequal variances; etc. of two-sample t-test, which assumes that the two sets of data are independent. Dependent t-test for paired samples is also available. Since we use independent two-sample t-test with unequal sample size and unequal variances[17], the rest of them will be omitted for simplicity purposes.

Unequal variances t-test or Welch's t-test [17] widely implement in statistical analysis while comparing the mean difference significance of two groups of data under the situation of their variances are not equal. The t statistics can be calculated by

$$t = \frac{\bar{X}_1 - \bar{X}_2}{s_{\bar{\Delta}}}$$

where

$$s_{\bar{\Delta}} = \sqrt{\frac{s_1^2}{n_1} + \frac{s_2^2}{n_2}}$$

in which, s_i^2 is the unbiased estimator of the corresponding group of data, $s_{\bar{\Delta}}$ is not the pooled variance. Regarding the test statistics distribution for the purpose of significance testing, it roughly follows the ordinary Student's t-test with the degree of freedom:

$$d.f. = \frac{(\frac{s_1^2}{n_1} + \frac{s_2^2}{n_2})^2}{\frac{(\frac{s_1^2}{n_1})^2}{n_1-1} + \frac{(\frac{s_2^2}{n_2})^2}{n_2-1}}$$

3. PROBLEM DEFINITION

Definition 1 (Neural Decoding). *It is a mathematical mapping from brain activity to the outside world. In the sensory domain, the outside world consists of the received visual, auditory, or other sensory information. In the motor domain, the outside world consists of the state of the skeletomuscular system. This is the inverse of neural encoding, which maps the outside world to brain activity. Because signals about motor intention precede movement, decoding can be thought of as "mind-reading." Neuroscientists seek to predict an action as soon as it is intended before it ever takes place* [18].

We are researching the neurons because it tells us about ourselves and the structure of our or animal's thoughts, as well as progress the present artificial intelligence system, which may also emancipate labor power from repeated or time-consuming works in the future. Even though with the rapid development of both neuroscience and machine learning, these two fields have rare interactions. In studying neuron decoding, the researchers still use traditional methods [19], [20]. Hence, we involve deep learning algorithms into the study of neuroscience in order to further our understanding of our or animal's brain. Inspired by [21], the state-of-the-art deep learning approaches that specifically aim to solve time-series related problems, such as LSTM and GRU, indeed significantly outperform the traditional techniques, Wiener Filter, for example. We thus select LSTM and GRU as our primary experimental deep learning method. We also utilize Support Vector Machine, Random Forest, Naive Bayes as the benchmark to measure the interactive model performance.

4. METHODOLOGY

The *BiLSTM* and *BiGRU* model will be applied in our paper. It takes time-series data (usually embedding in Natural Language Processing) and feed the LSTM cell forward and backward simultaneously. The propagation flowing procedure is:

- We move from left to right, starting with the initial time step we compute the values until we reach the final time step
- We move from right to left, starting with the final time step we compute the values until we reach the initial time step

Fig. 2. *BiLSTM* cell [6]

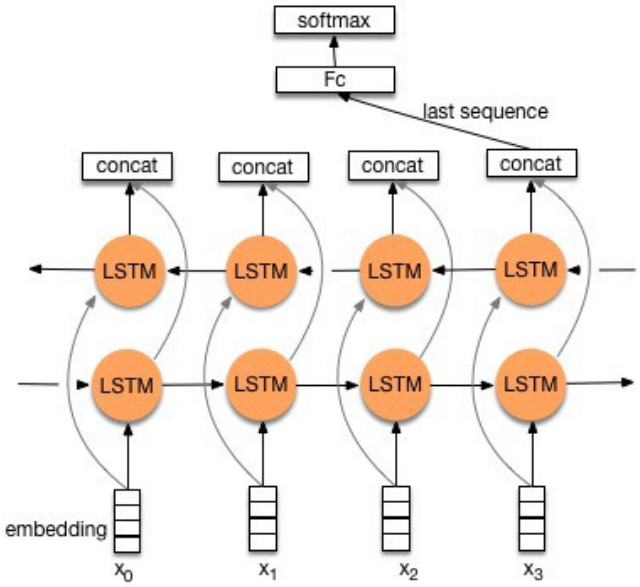

A. Data Collection and Outlook

Data collection is performed by a millisecond camera and a behavioral camera, for recording mouse neuron and motor behavioral, correspondingly. Before the experiment, researchers opened up a hole on the top of the mouse's head and fixed the millisecond camera in it. The camera recorded a fixed region of the hippocampus of the mouse brain and allowed itself to record the neuron activities by milliseconds. Another video recording machine, named the behavioral camera, was used to keep track of the motor activity of mice. The stored videos were saved as 250 X 443 for the behavioral camera, and 752 X 480 for the millisecond camera. Both had a frame rate of 30 frames/second. Videos for neural and behavioral activities contain information that is useful for decoding neurons. It is significant to extract these messages with a highly accurate technique, such as CNMF-E [22]. This method scans every frame of the video and detects the potential neurons from the frame by its luminance. Figure.3 is the original single video frame obtained from the millisecond camera recording. The implementation of CNMF-E labels each neuron based on their luminance (neural firing along with light), which is shown in Figure.4

B. Data Preprocessing

The neural activity data are extracted by CNMF-E [22] from the video recording of mouse hippocampus cortex firing state as input data for *BiLSTM*, along with the mouse location data processed by DeepLabCut [23] from the video recording of mouse motor activities in various experimental scenario as source of outputs.

The neural data and motor behavioral data were videotaped simultaneously, and the timestamp was documented as well, in which it helps to align the frame in neural activity and motor behavioral videos. There will be no mouse in the first few seconds of the motor behavioral video, be aware of clipping this part out of the entire analysis is vital to the veracity of the data.

Neural data generated by CNMF-E has to be transposed in order to feed one vector of neural activity for one specific time frame into the deep learning model, in our case, *BiLSTM* and

Fig. 3. Example of neurons in one single frame

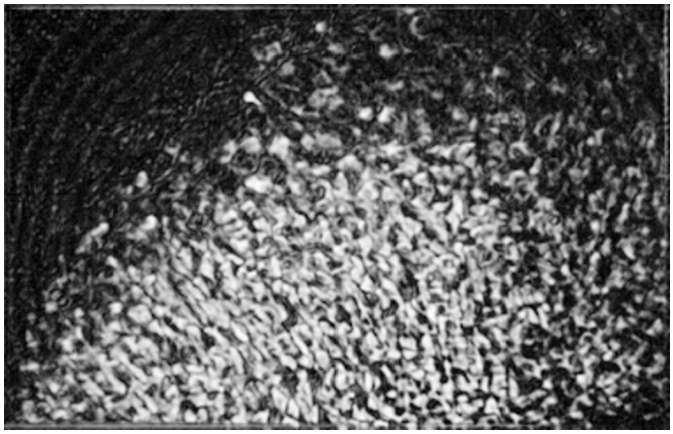

Fig. 4. Example of labeled neurons in one single frame

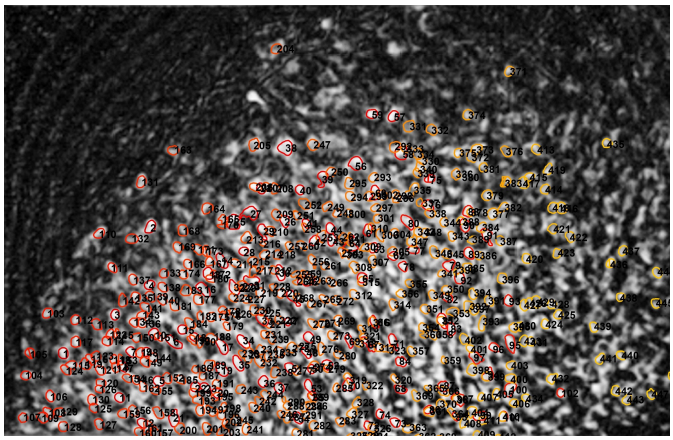

BiGRU. The output of the model is constructed by the calculation of the distance between bullying and defeated mice that was prepared by DeepLabCut. The distance is classified into two classes: less than 15 centimeter: two mice interacted; over 15 centimeters: no interaction. These two classes are the target that we would like to make the prediction. We determine the threshold as 15 centimeters because there is a highly likely chance that a defeated mouse is stressed by the bullying mouse under the distance of 15 centimeters [24]. In other words, stress is taking place while they are in the interaction zone (distance is less than 15 centimeter).

C. Model Architecture

Besides the following vanilla *BiLSTM* architecture, we add Dropout [25], [26] layer to prevent overfitting in training the network. Thus, we refer to Fig. 5 as the overall model architecture.

D. Model Parameters

After tuning the model to reach the its best performance, we are using hyper-parameters:

- *Activation function*: Softmax [27] transforms numbers or logits into probabilities that sum to one. The outputs of

Fig. 5. Overall Model Architecture

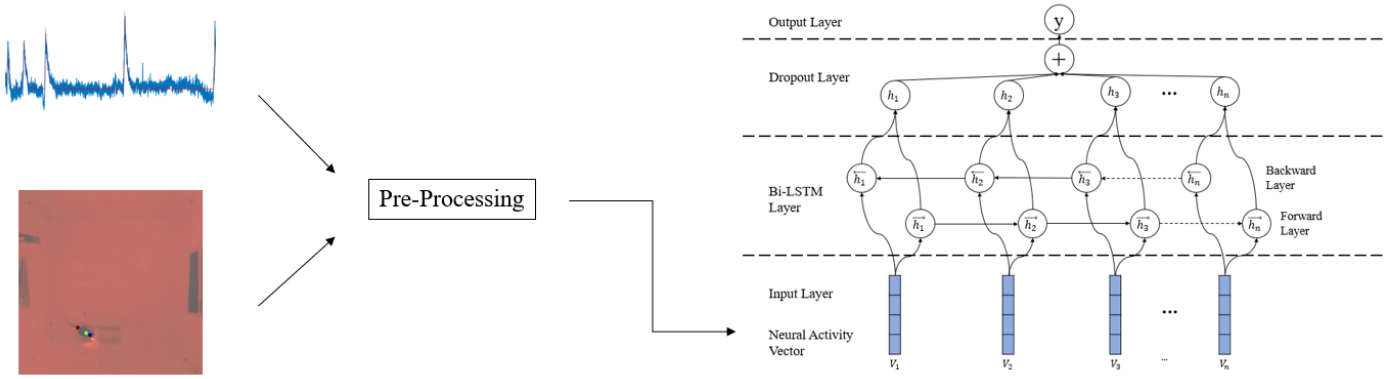

softmax function is a vector of a list of potential outcomes in terms of the probability distributions [28]. The standard softmax function is defined by the formula:

$$\sigma(\mathbf{z})_i = \frac{e^{z_i}}{\sum_{j=1}^{K} e^{z_j}} \; for\; i = 1, ..., K \; and \; \mathbf{z} = (z_1, ..., z_K)) \in \mathbb{R}^K$$

where z_i is each element of input vector $\mathbf{z}$. The sum of the output vector of softmax function is one, alternatively, each of component will be in the interval (0,1).

- *Optimization function*: Adam is a stochastic gradient-based optimization that aims to minimize the cost function, which is a guide for optimizer to change the weight to the right direction[29]. It outperforms significantly than the other traditional optimizer, such as Stochastic Gradient Descent or Momentum, in terms of computationally efficiency [30], [29] and training and validation loss reducing [31], [29]. We refer readers to the original paper [29] for more mathematical and structural details.
- *Learning rate*: we use 1e-4 as our initial learning rate.
- *Cost function*: we use cross entropy[32] as our cost function since the nature of the problem is classification [33].
- *Dropout rate*: We drop 0.3 portion of neurons during training session to avoid overfitting

5. EXPERIMENTS

The objectives of our experiments are to 1) evaluate the model accuracy, precision, and recall, 2) determine the mean difference significance between two different scenarios. The model is implemented in PyTorch [34] with the processor of Intel (R) Core (TM) i9-9980 XE CPU, 128 GB RAM, and one Nvidia GeForce RTX 2080 Ti graphics card.

A. Experiment Settings

We use three different experiment settings to evaluate our model and test the mean difference significance. Accuracy, Precision, and Recall of validation and Student's t-test p-value are the four main metrics that we take into considerations.

Dataset is a combination of input: neuron activity data and output: encoding with two mice distance less than or over 15 centimeters. The dataset is split into three groups: training, testing, and validation and the portion of each is 0.56, 0.3, 0.14, correspondingly.

Table 1. Statistics of datasets

	1058 SI A	1058 SI B	3470 SI A	3470 SI B	1056 SI A	1056 SI B
Interacted	2157	1876	809	304	2383	5447
Not interacted	7080	8880	3734	4232	6959	10722

SI scenario refers to the experiments were conducted at night, and the background color of the video is roughly red. Lights are not permitted to use during the experimental session. The objective is to eliminate the maximum level of noise from visual contact between two mice. *A* session represents that no bullying mouse presents in the experiment while *B* means the bullying mouse is in the enclosure and defeated mouse is able to smell its existence. The numbers, *1058*, for example, is the mouse annotated number for reference purpose.

B. Model Training & Metrics

The model follows the ordinary training procedure of deep learning model. With the defined activation function, optimizer, learning rate, and cost function, the bi-directional LSTM layer and dropout layer are applied to train the model. We consider our predictive model validation accuracy and loss as the metric to evaluate the model performance, which leads to the conclusions of how accurate this model correctly predicts the mouse social status (interacted or not), by given of a sequence of neural activity.

Moreover, we use Student's t-test to compare the mean difference significance between two groups of mouse neuron activity data. The primary setting of comparisons are

- Same scenario and mouse but the different session, 1056 SI A *verse* 1056 SI B, for instance, to determine if the presence of bullying mouse makes the significant impacts on defeated mouse's neuron activity.
- Same scenario, session, and mouse but different stress level, such as 1056 SI A interacted *verse* 1056 SI A no-interacted, for testing the mean difference significance of mouse's stress level.

Student's t-test is applied in accordance with the hypothesis:

- Null hypothesis H_0: mean of interacted neural activities = mean of no-interacted neural activities
- Alternative hypothesis H_1: mean of interacted neural activities $\neq$ mean of no-interacted neural activities

The test statistics and the p-value is used asover, we use Student's t-test t metrics. If the p-value is less than 0.05, we conclude that H_1 is highly likely to be accepted and H_0 is rejected.

C. Results

We use Student's t-test to determine the mean difference significance of neural activities and *BiLSTM* and *BiGRU* make the prediction of interaction between two mice.

C.1. Model Accuracy, Precision, and Recall

The model validation accuracy for different datasets are listed in Table 3 after converging. For the purpose of comparing these two RNN models: *BiLSTM* and *BiGRU*, the results are not significant to conclude which method is more suitable for neural decoding since both of them take equal frequency of highest accuracy among six datasets. However, it indeed implies that this general RNN model roughly has 0.985 chance to correctly tell us if the defeated mouse is interacting with bullying mouse, alternatively, whether this mouse is stressing or not.

Table 2. Model Accuracy

	1058 SI A	1058 SI B	3470 SI A	3470 SI B	1056 SI A	1056 SI B
BiLSTM (Ours)	0.974	0.982	**0.979**	**0.992**	0.984	**0.986**
BiGRU (Ours)	**0.976**	**0.983**	0.976	0.9918	**0.990**	0.985
SVM	0.921	0.910	0.956	0.975	0.912	0.934
Random Forest	0.931	0.933	0.965	0.955	0.932	0.946
Naive Bayes	0.755	0.762	0.698	0.768	0.723	0.776
LSTM-Softmax [35] Overall	0.652					
LSTM-SVM [35] Overall	0.664					

For simplicity purpose, we will not include all averaged precision and recall tables for every dataset. Instead, we selected *1056* mouse as our comparison because the distribution of *Interacted* and *Not interacted* is more balanced than others.

Table 3. Model Precision and Recall

	Precision	Recall
BiLSTM (Ours)	0.971	0.961
BiGRU (Ours)	**0.972**	**0.970**
SVM	0.962	0.901
Random Forest	0.970	0.921
Naive Bayes	0.802	0.655
LSTM-Softmax [35]	0.656	0.688

One epoch in the Fig 6 represents 200 epochs in the substantive training. Despite the accuracy of *BiLSTM* and *BiGRU* are approaching to the similar results as the increasing of epoch number, the time and speed of converging of *BiGRU* is more efficient than *BiLSTM* with the same hyperparameters. *BiLSTM* converges after approximately 500-600 epochs, while *BiGRU* takes 300-400 epochs to converge, which suggests that *BiGRU* is a preferred choice if the computational efficiency is the primary training consideration.

Fig. 6. Accuracy of *BiLSTM* and *BiGRU*

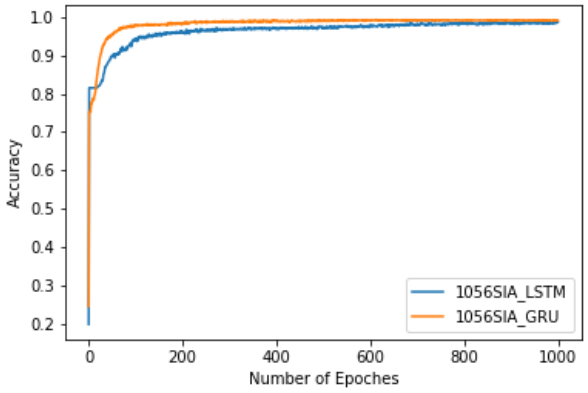

C.2. Student's t-test

We use the Student's t-test to determine the significance of the mean difference between two groups of neuron activities. The first setting is different stress levels (presence of bullying mouse), same mouse, session, and scenario in Table 4. There are two numbers in each cell and the former and latter represent the t-test results for non-interacted and interacted class, correspondingly. We found that all of the paired t-test p-values end up with *significant*, stating that the presence of bullying mouse is highly likely influencing the neuron activities of a defeated mouse. It also provides some clues about the stress level: the defeated mouse has relatively higher frequency of neuron activity when noticing the bullying appear in the enclosure, thus, taking considerations on the source of neuron activity data - hippocampus, which is the brain part related to the stress level of the animal [36], it suggests that the mouse's stress level increases when the thing that the defeated mouse is afraid of presents.

Table 4. Student's t-test across different stress level, same session, class and scenario

		1058SI	3470SI	1056SI
		A		
B	p-value	0; 0	0; 4.27e-25	0; 0
	Test Statistics	35.13; 26.9	70.76; 10.35	60.36; 111.44

Another experiment is conducted under the setting of the same mouse, session, and scenario, but different class, namely, interacted class *verse* non-interacted class, detailed in Table 5. As similar results with the previous test, all of the test is significant due to that the t-test p-value is less than 0.05, indicating that whether interacted with bullying mouse has a significant effect on defeated mouse neuron activity. However, one result is less significant than the others, which is 1058SI A. The p-value is 0.028 and it is close to our cut-off 0.05. We retrieve the session difference mentioned earlier, *A* means the bullying mouse is not shown up in the enclosure, whereas *B* describes the presence of bullying mouse. It statistically expresses that mouse 1058

has relatively low sensitivity to the enclosure, even though it is empty, but high sensitivity to the presence of bullying mouse because of the significance of t-test of 1058SI B. Mouse 1056 and 3470 have higher stress level to the enclosure no matter whether the bulling mouse shows up or not.

Table 5. Student's t-test across different session, same mouse and scenario

	1058 SI A	1058 SI B	3470 SI A	3470 SI B	1056 SI A	1056 SI B
p-value	0.028	6.68e-23	0	2.31e-56	0	3.25e-37
Test statistics	2.203	9.85	38.25	15.82	65.47	12.75

From an intuitive perspective, figure 7 explicitly demonstrates the neuron activity difference between bullying mouse presents and not, regarding the same scenario and mouse. The neuron activity figure suggests that the defeated mouse will have more neurons spiked when it has a vision on the bullying mouse than the case of non-presence of bullying mouse, which has shown that the defeated mouse is highly likely more stressed during the time of presence of bullying mouse.

Fig. 7. Intuitive comparison of number of neurons spiked for bullying mouse present or not

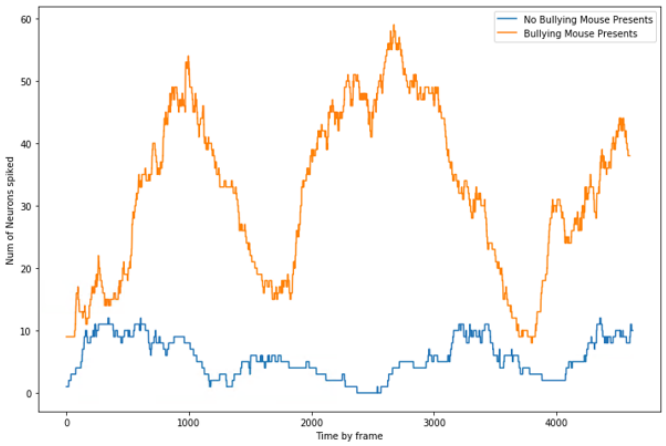

6. DISCUSSION

In this paper, we propose a deep learning-based stress determiner on hippocampus neural decoding and statistically prove the significance between two groups of neuron activities' mean value regarding the setting of the different session, same mouse and scenario, as well as different stress level, same mouse, scenario and session. The overall prediction accuracy is above 0.985, which outperforms other traditional machine learning models. All Student's t-test results are significant, concluding that the mean of our experimented groups is different. It also demonstrates that the presence of a bullying mouse and whether the defeated mouse is physically in the interaction zone make significant impacts on the defeated mouse's neuron activities.

In future work, in order to improve the interpretability, we may add an attention layer and feedforward neuron network to our architecture [37]. We exclude the feature engineer part from our study due to lack of time, it may be beneficial to the model performance if we extract the importance of each neuron and remove the ones that are not significant to the model because they bring the noise to the training process.

Because of the limited dataset size, *BiLSTM* may not reach its best performance. We hence consider merging the neuron activity data from the different sessions but the same mouse and scenario into one big dataset by aligning the neurons to expanding our training set. The merging algorithm is contributed by [24] but yet to test. Besides combining different sets of data, we may use an approach named oversampling [38]. We oversample the relative minority class of dataset, in our case, interaction class, until achieving the balance between interaction and not-interaction class, the model is hereby able to reach better performance [39]. An advanced variant of oversampling is Synthetic Minority Over-Sampling Technique (SMOTE) [39], which creates the new observation based on its nearest neighbor of a randomly selected point instead of sampling the existing data point in vanilla oversampling method, helps the model avoid overfitting and get better results [40].

Place cell [41], [42] may turn out to be a potential influential factor in model training of neuron activity. The group of neurons spikes is not only because of stress but also likely due to place cell. Thus, it confuses the model if the place cell neurons spike where no stress occurs. As reference from [24], one possible way to address this problem is to decrease the distance threshold from 15 centimeters to 10 centimeters, which is the direction of the future work.

We also intend to apply the deep learning model to the various scenario of the mouse experiments, Def, Hab, etc., for instance, to discover the feasibility of deep learning in neural decoding. As both of the defeated and bulling mice are free to move inside the cage in these scenarios, the distance calculation is varied, as well as model performance and other potential impact points.

7. ACKNOWLEDGEMENTS

The author thanks Prof. Benjamin Fung for long-time collaboration and engaging discussions, which were instrumental in providing helpful critique and valuable comments, as well as for his encouragement and support. Tremendous gratitude is expressed to Dr. Wong and Amanda Larosa for clarifying the key directions and concepts.

REFERENCES

1. S. Hochreiter and J. Schmidhuber, "Long Short-term Memory," Neural computation **9**, 1735–80 (1997).
2. K. Greff, R. K. Srivastava, J. Koutnik, B. R. Steunebrink, and J. Schmidhuber, "LSTM: A Search Space Odyssey," IEEE Transactions on Neural Networks and Learning Systems **28**(10), 2222–2232 (2017). URL http://dx.doi.org/10.1109/TNNLS.2016.2582924.
3. Y. Li, Z. Zhu, D. Kong, H. Han, and Y. Zhao, "EA-LSTM: Evolutionary Attention-based LSTM for Time Series Prediction," CoRR **abs/1811.03760** (2018). 1811.03760, URL http://arxiv.org/abs/1811.03760.
4. G. Petneházi, "Recurrent Neural Networks for Time Series Forecasting," (2019). 1901.00069.
5. Y. Hua, Z. Zhao, R. Li, X. Chen, Z. Liu, and H. Zhang, "Deep Learning with Long Short-Term Memory for Time Series Prediction," (2018). 1810.10161.
6. M. Schuster and K. Paliwal, "Bidirectional recurrent neural networks," IEEE Transactions on Signal Processing **45**(11), 2673–2681 (1997).
7. S. Siami-Namini, N. Tavakoli, and A. S. Namin, "A Comparative Analysis of Forecasting Financial Time Series Using ARIMA, LSTM, and BiLSTM," (2019). 1911.09512.

8. M. Nguyen, "Illustrated Guide to LSTM's and GRU's: A step by step explanation," (2019). URL https://towardsdatascience.com/illustrated-guide-to-lstms-and-gru-s-a-step-by-step-explanation-44e9eb85bf21.
9. G. Wang, W. Wei, J. Jiang, C. Ning, H. Chen, J. Huang, B. Liang, N. Zang, Y. Liao, R. Chen, and et al., "Application of a long short-term memory neural network: a burgeoning method of deep learning in forecasting HIV incidence in Guangxi, China," (2019). URL https://www.ncbi.nlm.nih.gov/pmc/articles/PMC6518582/.
10. J. Chung, C. Gulcehre, K. Cho, and Y. Bengio, "Empirical Evaluation of Gated Recurrent Neural Networks on Sequence Modeling," (2014). 1412.3555.
11. B. E. Boser, I. M. Guyon, and V. N. Vapnik, "A training algorithm for optimal margin classifiers," in *Proceedings of the fifth annual workshop on Computational learning theory*, pp. 144–152 (1992).
12. L. Breiman, "Random forests," Machine learning **45**(1), 5–32 (2001).
13. J. R. Quinlan, "Induction of decision trees," Machine learning **1**(1), 81–106 (1986).
14. L. Breiman, "Bagging predictors," Machine learning **24**(2), 123–140 (1996).
15. I. Rish *et al.*, "An empirical study of the naive Bayes classifier," in *IJCAI 2001 workshop on empirical methods in artificial intelligence*, vol. 3, pp. 41–46 (2001).
16. Student, "The Probable Error of a Mean," Biometrika **6**(1), 1–25 (1908). URL http://www.jstor.org/stable/2331554.
17. B. L. WELCH, "THE GENERALIZATION OF 'STUDENT'S' PROBLEM WHEN SEVERAL DIFFERENT POPULATION VARLANCES ARE INVOLVED," Biometrika **34**(1-2), 28–35 (1947). http://oup.prod.sis.lan/biomet/article-pdf/34/1-2/28/553093/34-1-2-28.pdf, URL https://doi.org/10.1093/biomet/34.1-2.28.
18. P. Wallisch, *Matlab for Neuroscientists*, 2nd ed. (Academic Press., 2014).
19. C. d'Avignon and D. Geman, "Tree-Structured Neural Decoding," Journal of Machine Learning **4**, 743–754 (2003).
20. R. Wang, X. Lou, B. Jiang, W. Cheng, X. Zheng, and S. Zhang, "Neural decoding using local field potential based on partial least squares regression," 2011 Annual International Conference of the IEEE Engineering in Medicine and Biology Society (2011).
21. J. I. Glaser, A. S. Benjamin, R. H. Chowdhury, M. G. Perich, L. E. Miller, and K. P. Kording, "Machine learning for neural decoding," (2017). 1708.00909.
22. P. Zhou, S. L. Resendez, J. Rodriguez-Romaguera, J. C. Jimenez, S. Q. Neufeld, A. Giovannucci, J. Friedrich, E. A. Pnevmatikakis, G. D. Stuber, R. Hen, and et al., "Efficient and accurate extraction of in vivo calcium signals from microendoscopic video data," eLife **7** (2018).
23. A. Mathis, P. Mamidanna, K. M. Cury, T. Abe, V. N. Murthy, M. W. Mathis, and M. Bethge, "DeepLabCut: markerless pose estimation of user-defined body parts with deep learning," Nature Neuroscience **21**(9), 1281–1289 (2018).
24. T. P. Wong, "The Douglas Research Centre," URL https://douglas.research.mcgill.ca/tak-pan-wong.
25. G. E. Hinton, N. Srivastava, A. Krizhevsky, I. Sutskever, and R. R. Salakhutdinov, "Improving neural networks by preventing co-adaptation of feature detectors," (2012). 1207.0580.
26. N. Srivastava, G. Hinton, A. Krizhevsky, I. Sutskever, and R. Salakhutdinov, "Dropout: A Simple Way to Prevent Neural Networks from Overfitting," Journal of Machine Learning Research **15**, 1929–1958 (2014). URL http://jmlr.org/papers/v15/srivastava14a.html.
27. C. M. BISHOP, *PATTERN RECOGNITION AND MACHINE LEARNING* (SPRINGER-VERLAG NEW YORK, 2016).
28. B. Gao and L. Pavel, "On the Properties of the Softmax Function with Application in Game Theory and Reinforcement Learning," (2017).
29. D. P. Kingma and J. Ba, "Adam: A Method for Stochastic Optimization," (2014). 1412.6980.
30. S. Bock, J. Goppold, and M. Weiß, "An improvement of the convergence proof of the ADAM-Optimizer," (2018). 1804.10587.
31. T. Dozat, "Incorporating nesterov momentum into adam," (2016).
32. G. E. Nasr, E. A. Badr, and C. Joun, "Cross Entropy Error Function in Neural Networks: Forecasting Gasoline Demand," in *Proceedings of the Fifteenth International Florida Artificial Intelligence Research Society Conference*, pp. 381–384 (AAAI Press, 2002). URL http://dl.acm.org/citation.cfm?id=646815.708603.
33. S. Mannor, D. Peleg, and R. Rubinstein, "The Cross Entropy Method for Classification," in *Proceedings of the 22Nd International Conference on Machine Learning*, ICML '05, pp. 561–568 (ACM, New York, NY, USA, 2005). URL http://doi.acm.org/10.1145/1102351.1102422.
34. A. Paszke, S. Gross, F. Massa, A. Lerer, J. Bradbury, G. Chanan, T. Killeen, Z. Lin, N. Gimelshein, L. Antiga, *et al.*, "PyTorch: An imperative style, high-performance deep learning library," in *Advances in Neural Information Processing Systems*, pp. 8024–8035 (2019).
35. H. Han, K. Byun, and H.-G. Kang, "A Deep Learning-Based Stress Detection Algorithm with Speech Signal," in *Proceedings of the 2018 Workshop on Audio-Visual Scene Understanding for Immersive Multimedia*, AVSU'18, p. 11–15 (Association for Computing Machinery, New York, NY, USA, 2018). URL https://doi.org/10.1145/3264869.3264875.
36. E. J. Kim, B. Pellman, and J. J. Kim, "Stress effects on the hippocampus: a critical review," Learning & memory **22**(9), 411–416 (2015).
37. M. Q. Li, B. C. M. Fung, P. Charland, and S. H. H. Ding, "I-MAD: A Novel Interpretable Malware Detector Using Hierarchical Transformer," (2019). 1909.06865.
38. J. Miao, J. Kirz, and D. Sayre, "The oversampling phasing method," Acta Crystallographica Section D: Biological Crystallography **56**(10), 1312–1315 (2000).
39. N. V. Chawla, K. W. Bowyer, L. O. Hall, and W. P. Kegelmeyer, "SMOTE: Synthetic Minority Over-sampling Technique," Journal of Artificial Intelligence Research **16**, 321–357 (2002). URL http://dx.doi.org/10.1613/jair.953.
40. G. E. A. P. A. Batista, R. C. Prati, and M. C. Monard, "A Study of the Behavior of Several Methods for Balancing Machine Learning Training Data," SIGKDD Explor. Newsl. **6**(1), 20–29 (2004). URL http://doi.acm.org/10.1145/1007730.1007735.
41. J. Okeefe and J. Dostrovsky, "The hippocampus as a spatial map. Preliminary evidence from unit activity in the freely-moving rat," Brain Research **34**(1), 171–175 (1971).
42. M.-B. Moser, D. C. Rowland, and E. I. Moser, "Place cells, grid cells, and memory," Cold Spring Harbor perspectives in biology **7**(2), a021,808 (2015).